Geochemistry and tectonic significance of the amphibolites of Etalin Formation in Trans Himalayan Belt, Arunahcal Pradesh, India

Debapriya Adhikary [1], Sebabrata Das [2], Chinchu S.V. [1]

[1] Geological Survey of India, NCEGR, Faridabad, Haryana,
[2] Geological Survey of India, DGCO, New Delhi,
India.

Published In IJIRMPS (E-ISSN: 2349-7300), Volume 12, Issue 3, (May-June 2024)

Abstract

On the basis of lithological variation and mineralogical variation, depending on relative proportion of hornblende, quartz and mica content, the Etalin Formation has been subdivided into four members viz Hornblende chlorite schist, Banded hornblende chlorite schist, Quartzite and Carbonatite with CaO content varies from 29.8 wt% to 41.65 wt%. The poikiloblastic texture of garnet and hornblende and the random orientation of hornblende laths is suggestive of their formation due to contact metamorphism and is attributed to intrusive nature of Lohit Granitoid with in the Etalin Formation. The lateral extent of different members in the eastern side is inferred and extrapolated due to complete inaccessibility of the area. The quartzite bands do not have much lateral extent towards west and it can be inferred that they exist as isolated patches. The presence of laths of hornblende in the banded hornblende chlorite schist member which are found to be floating in the mass of quartz and mica, may have formed in phase of retrogression. Chemical analysis of major oxides indicates that the composition of hornblende chlorite schists and banded hornblende chlorite schists is basaltic to dacitic, calc-alkaline and metaluminous. Trace element concentration indicates that these are calc-alkaline basalts which indicate volcanic arc setting. Mineral chemistry of Etalin Formation also suggests that the protolith is basic in nature.

Keywords: Mineral Chemistry, Amphibolite, Etalin Formation

Introduction

The Arunachal Himalaya occupies the easternmost part of the great Himalayan mountain range. The area studied belongs to the part of eastern Arunachal Pradesh also known as the Lohit Himalaya. This part shows some peculiarities in comparison to rest of the Himalaya. The major tectonic unit shows bend in their regional strike from NE-SW to NW-SE and this bend is known as Eastern Himalayan Syntaxis (EHS), which represents a major antiformal structure known as Siang antiform (Singh, 1993) or the Siang Window. The present area of study is part of eastern limb of the EHS. The region is considered to be part of central Burmese plate which abuts against the Indian plate along the Tiding suture (Nandy, 1980).

The study area mainly comprises rocks of Etalin Formaton and the Lohit Granitoids (Figure 1) which together are often called as the Lohit Granitoid Complex (LGC). In the present study attempts have been made to classify the different amphibolites constituting this Etalin Formation**.** In the study area Etalin Formation comprises dominantly of hornblende chlortie schist, banded hornblende chlorite schist, patches of carbonatite and quartzite. Present study is only concentrated on the classification of amphibolites of the Etalin Formation. The amphibolite classified below on the basis of field evidence, geochemistry and the petrographic study. Amphibolite Schist is the main rock type occurring in the north of the Lohit Crystalline Complex or the Lohit Granitoid, trending NW-SE dipping moderately to steep in NE & SW direction. It is well exposed along the Hayuliang–Goiliang and Hayuliang-Metangliang-Methumna road sections. Megascopically, it is a greenish grey coloured rock comprising persistent band of amphibole rich and felsic rich layers. Colour varies on the basis of dominance of mafic minerals. The rock shows megascopically and microscopically well developed schistossity**,** which is defined by hornblende and quartz rich layers**.** Banded amphibolite Schist is exposed along the Hayuliang-Goiliang and Hayuliang-Metangliang road sections. The rock is greyish-green to bottle green in colour, medium grained, mostly fine grained, trending NW-SE with steep dip towards NE-SW. The outcrop shows well developed parallel arrangements of compositional colour bandings. They show alternate bands like thin lamellae of amphibole and silica rich layers. This parallel arrangement gives a defused layered look to the rock which may also be transposed bedding. The parallel arrangement imparts schistosity to the rock. This rock type occupies vast stretch around Gimliang and Tamlavgan village and forms steep escarpment face of the hills and forms steep high hills**.**

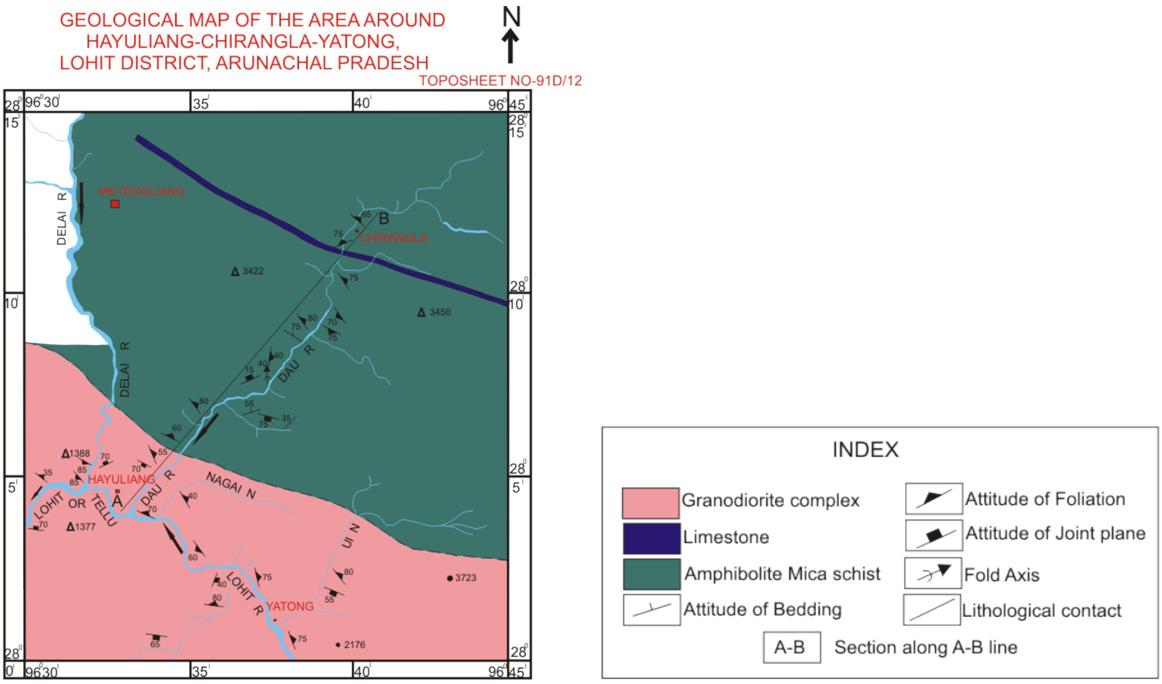

Figure 1: Geological Map of the Area around Hayuliang-Chirangla-Yatong, Lohit District, Arunachal Pradesh (Kirmani et. al., 1987)

Regional Structure

Due to extreme remoteness, inaccessibility, hostile terrain and dense vegetation most of the area still remains out of reach for detailed geological study and overall the geological data on this crucial segment still remains limited. However the best possible structural element was recorded in the mapped area. Bedding were very rare to get in this area it is developed in quartzites and in schistose rocks the parallel alternate arrangement of biotite, chlorite, hornblende and quartz and feldspar wherever are rich in silica grains impart a diffused layered look (compositional colour banding) which may also be transposed foliation. The general trend of rocks is NW-SE with moderate to steep dip towards NE. It is well exposed in Hayuliang Goiliang section. The area has undergone 3 generation of folding. The F2 folds are the most dominant fold pattern observed in the area. The second generation folds (F2) are co-axial with F1 folds. The first generation of folding is represented by very tight to isoclinals folds. The intensity of deformation was very high as the imprints of F1 folding is also observed in Lohit granitoids as well as the second generation of folding which is dominant over the area. The second generation folding is manifested by M-Z type S type, Hook shaped folds and other types of fold. The F2 folding is the most pervasive folding observed in the area, trend28 of which is NW-SE with moderate to steep dip towards NE. The second generation fold (F2) becomes co-axial with F1 folds with progressive deformation and forms the dominant foliation pattern in the area which is NW-SE with moderate to steep dip towards NE. The coaxial F1 and F2 folding pattern gives a layer of alternate light colour silica rich and mafic rich layers. The third generation of fold is observed in the form of broad warps and open fold trends NE-SW with moderate dip towards NW and SE. Other deformational features observed in the area are boudins, related with folds of flexure slip where the stretching of outer layer in the hinge zone is accommodated by pull apart of beds and formation of boudins. Faults are observed within hornblende chlorite schist of Etalin Formation mainly near Bomlan village. The orientation of the fault plane is 310 dipping at an angle of 30 towards NE. These are intra-formational faults. Thick quartz veins are also marked along these fault planes. Stretching along these planes results in boudin formation.

Detailed Study of Etalin Amphibolite Petrography

Amphibolite Schist mainly composed of hornblende, quartz, plagioclase garnet, chlorite, apatite and epidote with minor amount of biotite and muscovite (Figure 2). Schistosity is defined by the alignment of hornblende (Figure 3) and chlorite alternating with quartz and feldspar rich layer. Due to intense deformation suffered by the rock, many small scale micro folds are observed (Figure 4). Subhedral to euhedral grains of quartz are present at the hinge and elongated quartz grains are present at the limb of the microfolds. Occurrences of garnets are well recorded both in hand specimen and in petrographic study in Hayuliang Goiliang section as well as in Hayuliang Methumna section. In Hayuliang Goiliang section, garnets are euhedral in shape with well defined grain boundary along which chloritisation takes place. Many quartz inclusions are present within the garnet porphyroblast and chloritisation also takes place along the fractures within the garnet (Figure 5). Garnets are not deformed which indicates that these are post tectonic garnets and chloritisation along the grain boundary indicates that these are the product of retrogression. Near Methumna village in Hayuliang Methumna section, garnets porphyroblasts are fractured, chloritised and deformed, and have developed adjacent to the silica rich veins. Chlorite and muscovite swerves along these garnets which indicate that these are pre-tectonic. These garnets probably formed due to the injection of later stage fluid that brings sufficient amount of heat to mobilise the ferromagnesian minerals adjacent to it, which triggers the formation of garnets. Muscovites are also recorded in minor amount which does not exhibit any kind of foliation or schistossity. Within a deformed terrain, random orientation of muscovite signifies that these are secondary product and are not genetically related to the bulk composition. Apatite and epidotes are also present but spatially there occurrences are observed near the contact of the Granodiorite-diorite body and Hornblende-chlorite schist. Apatite and epidotes have well developed grain boundaries and are not deformed. These are secondary minerals and can be related with the intrusion of Granodiorite-diorite body.

Overall texture of the rock is dominantly rich in hornblende and chlorites which are prismatic and needle like minerals, respectively. Growth rate of these minerals are maximum in the direction perpendicular to the maximum principal stress and will grow rapidly than those with other orientation (Philpotts, R. A., 1989). Due to this reason hornblende and chlorite grows rapidly and forms elongated euhedral and larger crystals and imparts a schistosity in rock with progressive deformation. The rock contains porphyroblasts of garnet. The porphyroblasts contain inclusions of quartz within it which defines poikiloblastic texture of the rock. Overall the texture of the rock may be defined as schist with poikiloblastic garnet.

Banded amphibolite Schist rock is composed of amphiboles mostly hornblendes and ortho-amphiboles, chlorite, plagioclase, epidote and very minor amount of biotite, muscovite and dolomite. Thin alternate lamellas of silica and amphibole are present. The rock is well deformed and crenulations cleavages are also present which is defined by biotite, where early schistosity is bent into sigmoid curves by the later crenulation schistossity. Within the bends the amount of quartz is subsequently less than the surrounding rocks, presumably as a result of removal by solution. This results in the crenulation schistossity being marked by mica rich layers (Philpotts, R. A., 1989). Near Gimliang village, the rock exhibits a typical distinctive character, having elongated laths of hornblendes of 1-7 cm. The larger prismatic crystals of hornblende are randomly oriented and segregated along with muscovite in thin layers alternating with quartz dominant layers which also contains hornblende. Microscopically the prismatic crystals of hornblende having sharp boundaries are floating in the finer matrix of quartz and muscovite. The hornblende grains show cross cutting relationship with each other and the prismatic crystals also contains inclusion of quartz within it, which signifies rapid growth of hornblende porphyroblast. This may be attributed to secondary growth and can be related to different deformation stages or intrusive episodes of Lohit Granitoids. Overall texture of the rock contains subhedral grains indicating hybidioblastic texture. The most prominent fabric the rock has developed is gneissosity, which is defined by granular minerals and compositional layering of biotite rich layers (forms crenulations) and quartzo-feldspathic layers. Inclusion of quartz in hornblende indicates poikiloblastic texture which indicates rapid growth of hornblendes under high energy condition. So, texturally the rock can be named as hybidioblastic gneiss with hornblende poikioloblast.

Figure 2: Stretched Quartz Grains and Foliation in the Hornblende Chlorite Schist. Loc: Few Kilometres before Gimliang Village

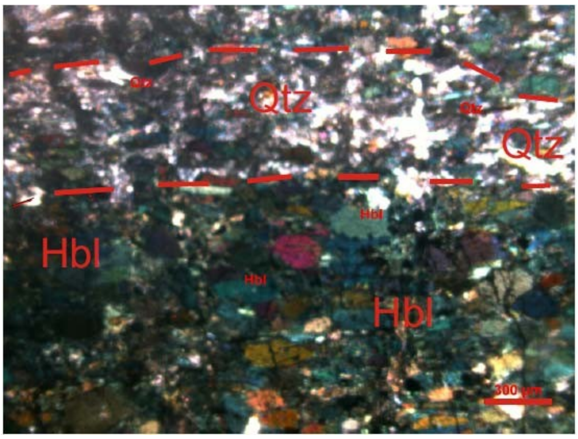

Figure 3: Photomicrograph of Hornblende-chlorite Schist Showing Well-defined Foliation. Loc: Few Kilometres before Gimliang Village

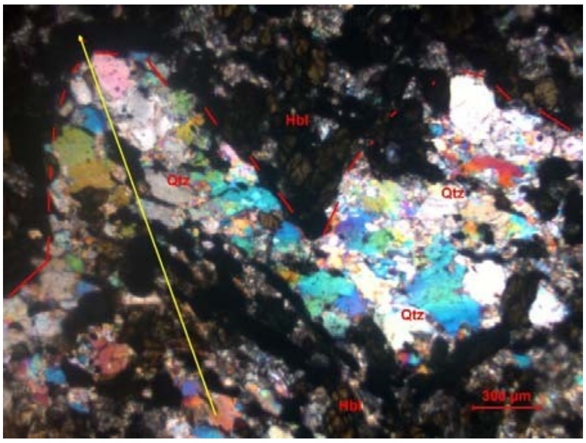

Figure 4: Photomicrograph Showing Microfold with Subhedral to Euhedral Quartz Grains at the Hinge. Loc: In-between Tamlavgam and Goiliang Village.

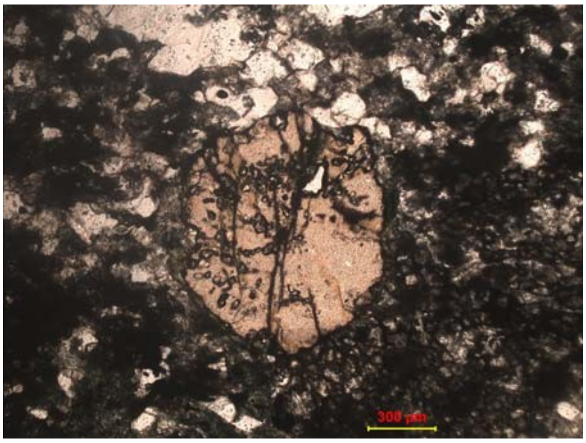

Figure 5: Photomicrograph Showing Euhedral Garnet Crystal with Inclusion of Quartz and Mica and Chloritization along the Grain Margin. Loc: In-between Tamlavgam and Goiliang Village.

Geochemistry and Tectonic Environment

Selected samples from the amphibolites of Etalin Formation are used for the evaluation of the geochemical characteristics of these rocks.

Hornblende chlorite schist is the main rock type occurring in the north of the Lohit Crystalline Complex or the Lohit Granitoid, trending NW-SE dipping moderately to steep in NE direction and it also shows SW direction where it has folded. It is well exposed along the

Hayuliang–Goiliang and Hayuliang-Metangliang-Methumna road sections. The presence of tongues and apophyses of granodiorite within this rock type points to the intrusive nature of the granitoids within these rocks. Concentration of major oxides (in wt%) such as SiO2, Al2O3, Fe2O3(T), Na2O, CaO, K2O, MnO, MgO and P2O5 varies (Annexture:1) in ranges from 44.98-72.28, 11.61- 17.57, 0.69-12.45, 1.14-5.2, 1.87-9.14, 0.34-3.24, 0.01-0.26, 0.35-12.09 and 0.04-0.51, respectively. A, C and F components [where A = Al2O3 + Fe2O3 – Na2O – K2O, C = CaO – 3.3 * P2O5 and F = FeO + MnO + MgO] were recalculated on the basis of 100 wt% and there values varies from 19.25-50.46, 14.50-40.5 and 13.71-58.38, respectively. Among trace element concentration (in ppm) Ni, Sr, V and Zr shows significant range in values i.e. 17-176, 86-875, 127-650 and 27- 382, respectively.

Banded hornblende chlorite schist is exposed along the Hayuliang-Goiliang and Hayuliang-Metangliang road sections. The rock is greyish-green to bottle green in colour, medium to fine grained, trending NW-SE with steep dip towards NE-SW. The outcrop exhibits well developed parallel arrangements of compositional bandings. They show alternate bands like thin lamellae of amphibole and silica rich layers. This parallel arrangement gives a defused layered look to the rock which may also be transposed bedding. The parallel arrangement imparts schistosity to the rock. This rock type occupies vast stretch around Gimliang and Tamlavgan village and forms steep escarpment face of the hills and forms steep high hills**.** Concentration of major oxides (in wt%) such as SiO2, Al2O3, Fe2O3(T), Na2O, CaO, K2O, MnO, MgO and P2O5 varies in ranges from 29.19-67, 9.29-18.6, 4.4-9.35, 0.22-4.03, 4.38- 27.35,0.12-4.3, 0.07-0.24, 2.58-8.4 and 0.1-0.34, respectively. A, C and F components [where A = Al2O3 + Fe2O3

– Na2O – K2O, C = CaO – 3.3 * P2O5 and F = FeO + MnO + MgO] were recalculated on the basis of 100% and there values varies from 11.59-29.33, 30.76-62.96 and 25.4-41.3, respectively. There is no significant concentration of trace elements are observed except Ni and V which shows a range in values from 15-126 ppm and 31-435 ppm, respectively. Hornblende chlorite schist of Etalin Formation were plotted on total alkali vs silica diagram and classified as basalt-basaltic andesite-andesite after Le Bas et al*.,* 1986 (Figure 6). The rocks of Etalin Formation show calc alkaline nature when plotted in AFM diagram (after Irvin and Barager, 1971) (Figure 7). According to Shand's Index 1943, the composition of Etalin Formation is dominantly metaluminous having A/NK value (molar) ranges from 1.4 to 2.45 and A/CNK value (molar) ranges from 0.17 to 1.17 (Figure 8). The peraluminous nature may be attributed to the presence Al in feldspars in hornblende chlorite schists of Etalin Formation. So, few samples plot in peraluminous field.

Trace elements discrimination diagram has been used to infer the tectonic environment of the rock. Rock of Etalin Formation were plotted in Hf/3-Th-Ta triangular diagram after Wood, 1980 and it plotted in D field which indicate that these are calc alkaline basalt (Figure 9). These calc alkaline basalts decipher the tectonic setting of theses basalts as volcanic arc setting. In multielement plot, elements are arranged into LILE group followed by HFSE group ultimately followed by transition element Ni and Cr, from left to right. These elements are normalised to MORB after Bevins et al*.,* 1984 (Figure 10). The pattern shows enrichment in LIL elements which may be due to the involvement of fluid phase and the enrichment of Th and Ba are indicative, but not diagnostic, of basalts that have experienced crustal contamination.

The REE data were normalised to MORB values after Taylor and McLennan, 1985 (Figure 11) and are presented on a concentration vs atomic number diagram. The REE pattern shows enriched LREE pattern with almost a linear trend from La-Nd with a moderate Eu anomaly whereas the HREE (Er to Lu) shows fractionated pattern. In few samples HREE shows linear pattern. Distribution pattern of REE exhibits medium to strongly fractionated pattern with (La/Yb)N ratio 1.56 to 12.83 with almost flat LREE pattern with (La/Sm)N ratio 0.55 to 1.61 and low to moderately enriched HREE pattern with (Tb/Yb)N ratio 0.98 to 4.28. The total average REE content is 57.14. REE pattern exhibits medium to strong Eu anomaly with Eu/Eu * value ranges from 0.71 to 0.15 which may be attributed to the presence of feldspar in the parent rock.

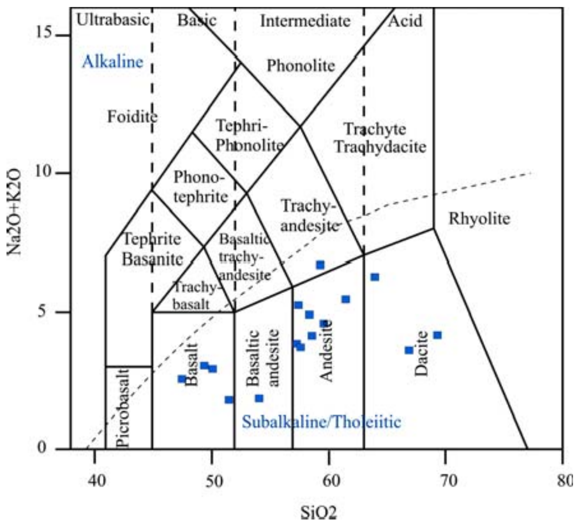

Figure 6: Discrimination Diagram of Showing Composition of Etalin Formation after Le Bas et al. 1986

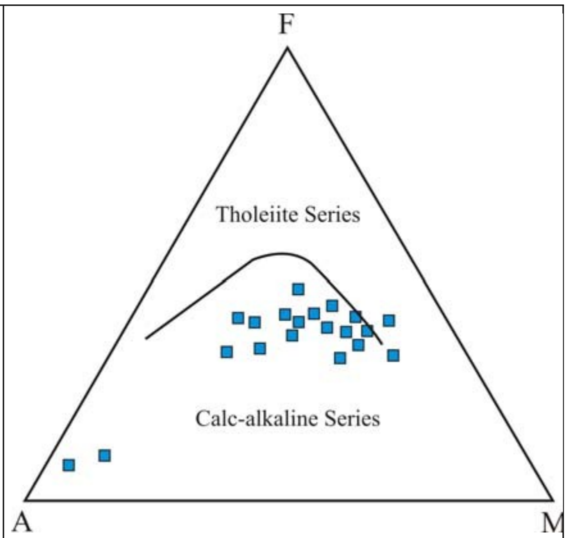

Figure 7: AFM Diagram Showing Calc Akaline Nature of Etalin Formation

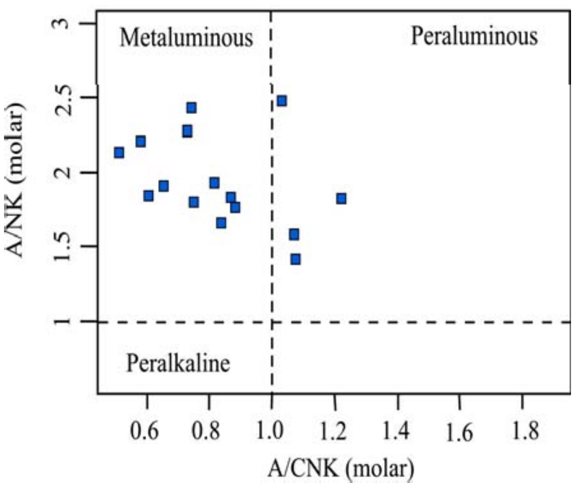

Figure 8: Diagram Showing Metaluminous Nature of Etalin Formation

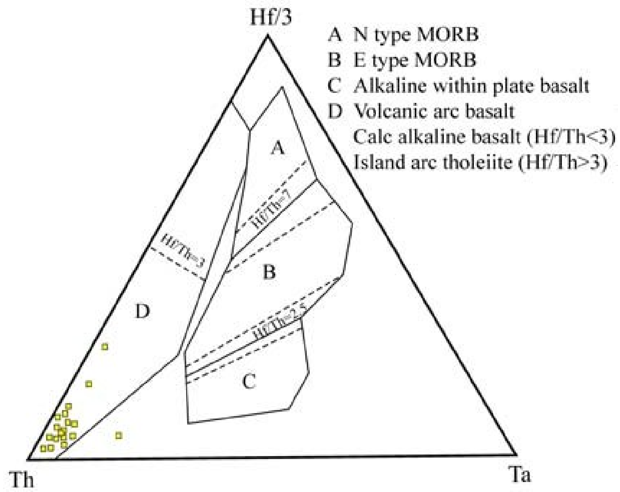

Figure 9: Discrimination Diagram Showing Calc Alkaline Basalt after Wood, 1980

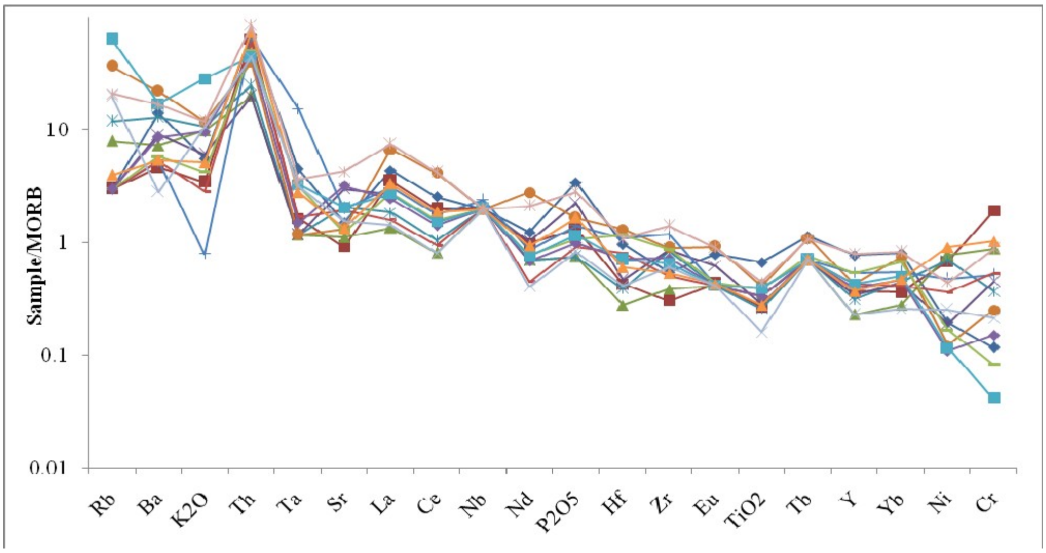

Figure 10: MORB normalised multi element plot of Etalin Formation after Bevins et al. 1984

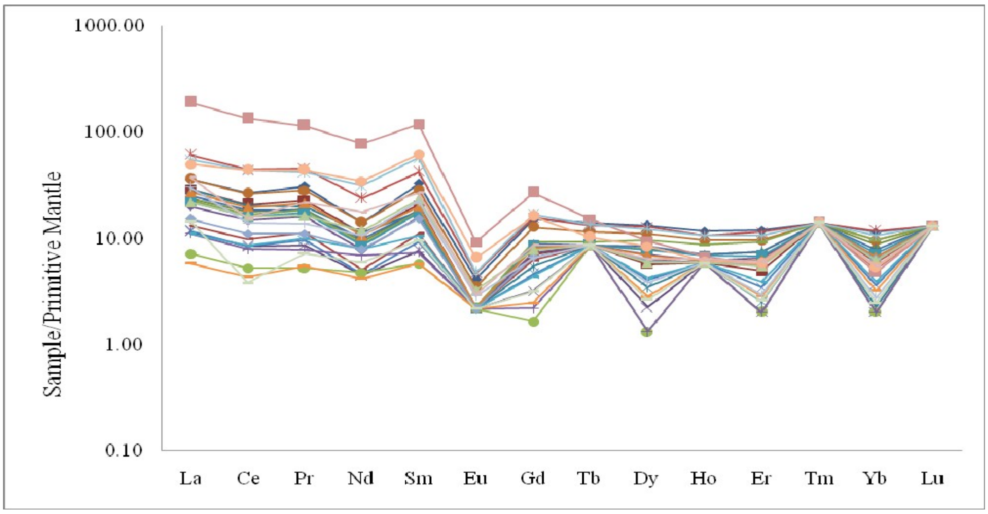

Figure 11: REE plot of Etalin Formation normalized to Primitive Mantle after Taylor and McLennan, 1985.

Annexure 1: Chemical Analysis of major oxides and trace elements pertaining to amphibolites of Etalin Formation

Sample No	AJ/12-13/HG/61	AJ/12-13/HG/62	AJ/13-14/HM/82	AJ/13-14/MC/112	AJ/13-14/MC/117	AJ/13-14/MC/122	AJ/12-13/HG/35
Lithology	Hbl-Chl-Schist	Hbl-Chl-Schist	Hbl-Chl-Schist	Hbl-Chl-Schist	Hbl-Chl-Schist	Hbl-Chl-Schist	Banded Hbl-Chl-Schist
Latitude	28° 09' 02.1"	28° 09' 10.3"	28° 07' 29.9"	28° 13' 16.1"	28° 13' 54.2"	28° 14' 29.6"	28° 06' 51.3"
Longitude	96° 39' 07.3"	96° 39' 11.7"	96° 32' 52.8"	96° 32' 55.5"	96° 32' 24.2"	96° 31' 56.5"	96° 35' 47.3"
SiO_2	54.95	70.75	55.55	58.88	61.4	72.28	64.77
TiO_2	0.43	0.15	0.6	0.62	0.55	0.07	0.6
Al_2O_3	12.07	15.19	11.61	13.51	14.97	14.84	10.24
Fe_2O_3 T	8.58	0.87	8.09	7.62	4.75	0.69	6
FeO	2.66	0.27	2.51	2.36	1.47	0.21	1.86
Fe_2O_3	5.92	0.60	5.58	5.25	3.28	0.48	4.14
MnO	0.17	0.01	0.14	0.13	0.07	0.05	0.1
MgO	6.88	0.8	8.66	5.07	2.9	0.35	5.41
CaO	8.67	2.54	6.67	4.51	5.03	1.87	6.14
Na_2O	2.74	5.2	3.52	3.39	4.46	4.74	3.31
K_2O	0.92	1.01	0.34	1.78	1.55	2.47	0.12
P_2O_5	0.27	0.07	0.09	0.2	0.25	0.04	0.17
Ba	110	299	69	265	252	774	63
Co	41	0	42	19	10	< 1	26
Cr	131	3	395	73	21	< 15	150
Cu	51	14	71	72	121	11	36
Ga	21	32	23	21	25	24	23
Nb	< 5	< 5	< 5	< 5	< 5	< 5	6
Ni	26	< 2	176	17	< 2	< 2	66
Pb	4	6	9	< 2	< 2	15	< 2
Rb	< 3	< 3	< 3	37	16	33	< 3
Sc	50	7	32	35	12	< 3.5	15
Sr	410	875	86	181	678	354	271

Th	< 4	< 4	9	8	5	8	13
V	291	< 20	330	311	182	< 20	129
Y	12	< 5	14	15	11	8	19
Zn	79	21	86	88	92	38	69
Zr	76	191	39	79	195	59	104
L.O.I. (%)	1.59	0.7	1.98	2.18	1.67	0.63	0.98

EPMA Analysis

The chemical composition of coexisting mineral phases in amphibolites schist & banded amphibolites schist of Etalin Formation was determined at the Northern Region, Petrological laboratory of G.S.I., Faridabad using CAMECA SX-100 microprobe. The operating conditions were 1micron beam diameters, 15 KV accelerating voltage and 12 nA beam current. The PAP matrix corrections were applied for analysing and natural silicate standards were used to quantify.

Garnet, biotite, amphibole, plagioclase feldspar are analysed (Annexture: 2, 3, 4 & 5) in the EPMA study from the amphibolites schist. Garnet in amphibolites schist is essentially an Almandine-Grossular solid solution with little amount of pyrope and spessartine contant. Andradite contant are insignificant in the rock. The porphyroblastic Gt (Figure 12) do not shows any chemical varying in terms of almandine and grossular contains from the core part of the grains to the rimal part, while pyrope contant also remains almost unaffected. All the Gt almandine amount are (Xalm = 0.55-0.61) and grossular content (Xgr = 0.15-0.25). Plagioclase feldspars occurring as isolated recrystallised grains have Xab varies in the range of 0.80-0.83. All the amphibole present in this rock is calcic group. One type calcic amphibole present here, this is magnesiohastingsite. In biotite grains XFe value ranges from 0.46 to 0.47 and XMg value ranges from 0.53 to 0.54.

Amphibole, plagioclase feldspar are analysed in the EPMA study from the banded amphibolites schist. All the amphibole present in this rock are calcic group. One type calcic amphibole present here, this is tschermekite. Plagioclase feldspars occurring as isolated recrystallised grains have Xab varies in the range of 0.72-0.74.So there is a distinct chemical composition different in the two types of amphibolites in the Etalin Formation.

Annexure 2: EPMA Data of clinopyroxene and cation calculated on the basis of 6 oxygen atom

Sample No.	**19A**	**19A**	**19A**	**19A**	**19A**	**19A**	**19A**	**19.00**	**14.00**	**14.00**
Points	12 / 1	16 / 1	26 / 1	39 / 1	41 / 1	45 / 1	46 / 1	18 / 1	16 / 1	17 / 1
SiO2	51.92	52.46	51.68	51.89	52.31	52.09	52.11	51.29	51.82	51.91
TiO2	0.13	0.26	0.25	0.36	0.25	0.22	0.26	0.31	0.39	0.30
Al2O3	2.06	2.08	2.09	2.08	2.01	2.04	2.08	2.08	1.85	1.77
Cr2O3	0.00	0.00	0.31	0.00	0.00	0.04	0.04	0.02	0.00	0.00
V2O3	0.00	0.00	0.00	0.00	0.00	0.00	0.00	0.00	0.00	0.00
Fe2O3	2.06	2.80	1.83	2.04	2.36	1.80	2.04	1.76	2.39	1.57

FeO	7.98	8.51	9.56	8.72	7.97	7.10	7.18	8.78	6.99	6.92
MnO	0.50	0.31	0.32	0.44	0.30	0.32	0.26	0.50	0.39	0.43
MgO	13.43	13.62	13.39	13.69	13.56	13.46	13.40	13.36	13.88	13.51
NiO	0.00	0.00	0.00	0.00	0.00	0.00	0.00	0.00	0.00	0.00
ZnO	0.00	0.00	0.07	0.00	0.00	0.00	0.04	0.00	0.00	0.00
CaO	21.78	21.63	20.78	21.21	22.34	22.62	22.70	20.82	22.15	22.73
Na2O	0.41	0.46	0.34	0.35	0.37	0.44	0.46	0.39	0.37	0.39
K2O	0.00	0.00	0.00	0.00	0.01	0.01	0.00	0.00	0.03	0.00
Total	100.26	102.14	100.62	100.78	101.46	100.14	100.56	99.31	100.25	99.52
Si	1.94	1.93	1.93	1.93	1.93	1.94	1.93	1.93	1.93	1.94
Ti	0.00	0.01	0.01	0.01	0.01	0.01	0.01	0.01	0.01	0.01
Al	0.09	0.09	0.09	0.09	0.09	0.09	0.09	0.09	0.08	0.08
V	0.00	0.00	0.00	0.00	0.00	0.00	0.00	0.00	0.00	0.00
Cr	0.00	0.00	0.01	0.00	0.00	0.00	0.00	0.00	0.00	0.00
Fe+3	0.06	0.08	0.05	0.06	0.07	0.05	0.06	0.05	0.07	0.04
Fe+2	0.25	0.26	0.30	0.27	0.25	0.22	0.22	0.28	0.22	0.22
Mn	0.02	0.01	0.01	0.01	0.01	0.01	0.01	0.02	0.01	0.01
Mg	0.75	0.75	0.75	0.76	0.75	0.75	0.74	0.75	0.77	0.75
Ni	0.00	0.00	0.00	0.00	0.00	0.00	0.00	0.00	0.00	0.00
Zn	0.00	0.00	0.00	0.00	0.00	0.00	0.00	0.00	0.00	0.00
Ca	0.87	0.85	0.83	0.84	0.88	0.90	0.90	0.84	0.88	0.91
Na	0.03	0.03	0.02	0.03	0.03	0.03	0.03	0.03	0.03	0.03
K	0.00	0.00	0.00	0.00	0.00	0.00	0.00	0.00	0.00	0.00
Total	4.00	4.00	4.00	4.00	4.00	4.00	4.00	4.00	4.00	4.00
XMg2+	0.75	0.74	0.71	0.74	0.75	0.77	0.77	0.73	0.78	0.78
XMgt	0.71	0.69	0.68	0.70	0.71	0.73	0.73	0.70	0.73	0.74
Ac	0.03	0.03	0.02	0.03	0.03	0.03	0.03	0.03	0.03	0.03
Jd	0.00	0.00	0.00	0.00	0.00	0.00	0.00	0.00	0.00	0.00
CrTs	0.00	0.00	0.01	0.00	0.00	0.00	0.00	0.00	0.00	0.00
AlCaTs	0.03	0.02	0.03	0.03	0.02	0.03	0.03	0.04	0.02	0.03
Wo	0.87	0.85	0.83	0.84	0.88	0.90	0.90	0.84	0.88	0.91
En	0.75	0.75	0.75	0.76	0.75	0.75	0.74	0.75	0.77	0.75
Fs	0.25	0.26	0.30	0.27	0.25	0.22	0.22	0.28	0.22	0.22

Annexure 3: EPMA Data of garnet and cation calculated on the basis of 6 oxygen atom

Sample No.	30	30	111	111	111
Points	6 / 1	7 / 1	1 / 1	2 / 1	3 / 1
SiO2	37.154	37.374	37.895	38.329	37.743
TiO2	0.295	0.094	0.234	0	0.141
Al2O3	20.789	20.658	20.847	21.02	20.618
Cr2O3	0	0	0	0.014	0
V2O3	0	0	0	0	0
Cr2O3	0	0	0	0.014	0
Fe2O3	1.2171857	0.4814975	0.1889894	-0.715674	1.3537333
FeO	26.514766	27.612744	26.322946	26.901969	26.406899
MnO	5.192	2.826	3.139	2.606	1.905
MgO	3.118	3.316	2.776	2.777	3.504
NiO	0	0	0	0	0
ZnO	0.074	0	0	0	0
CaO	5.694	6.424	8.559	8.851	8.155
Na2O	0	0.034	0.023	0	0.045
K2O					
Total	100.04795	98.820242	99.984935	99.783296	99.877633
Si	2.9673013	3.0039554	3.0072599	3.0388466	2.9918629
Ti	0.0177247	0.005684	0.0139703	0	0.0084086
Al	1.9567953	1.9568967	1.9497923	1.9641278	1.9262273
V	0	0	0	0	0
Cr	0	0	0	0.0008776	0
Fe+3	0.0731528	0.029123	0.0112861	-0.042699	0.0807526
Fe+2	1.770973	1.8561008	1.7469949	1.7837478	1.7506155
Mn	0.3512178	0.1923897	0.2109921	0.1750014	0.1279045
Mg	0.371228	0.397326	0.3284105	0.3282205	0.414074
Ni	0	0	0	0	0
Zn	0.004363	0	0	0	0
Ca	0.4872442	0.553226	0.727755	0.751877	0.6926317
Na	0	0.0052985	0.0035389	0	0.0069162
K	0	0	0	0	0.0006068
Total	8	8	8	8	8

Adr	0.0360368	0.014664	0.0057551	-0.022222	0.0402359
Py	0.1200572	0.1305415	0.1083291	0.1104085	0.1331267
Alm	0.5727427	0.6098223	0.5762618	0.600026	0.5628311
Grs	0.1575775	0.1817625	0.2400565	0.2529201	0.2226844
Spss	0.1135858	0.0632097	0.0695976	0.0588678	0.0411219

Annexure 4: EPMA data of amphiboles of Etalin Formation and cations recalculated on the basis of 23 oxygen atoms

Sample No.	**27**	**27**	**61**	**61**	**61**	**115**	**115**
Points	27-1/1.	27-2/1.	61-16/1.	61-25/1.	61-39/1.	115-1/1.	115-2/1.
SiO2	42.844	44.012	46.689	45.526	44.836	48.878	50.294
TiO2	0.916	0.267	0.592	0.7	0.658	0.483	0.254
Al2O3	13.755	13.759	9.403	11.452	11.086	8.379	7.258
FeO	14.821	14.383	13.461	13.963	14.337	8.06	8.2
MnO	0.256	0.347	0.136	0.28	0.277	0.148	0.145
MgO	10.763	10.452	12.723	11.525	11.803	17.575	17.502
CaO	11.027	11.092	11.539	11.271	11.733	11.531	11.957
Na2O	2.09	1.984	1.562	1.843	1.81	1.981	1.681
K2O	0.295	0.372	0.488	0.633	0.718	0.125	0.14
BaO	0	0	0	0.202	0.588	0	0.127
P2O5	0.069	0.032	0.017	0	0	0	0
Cr2O3	0	0.088	0.002	0.104	0.017	0.217	0.242
ZnO	0	0	0.07	0.037	0.043	0	0
F	0.162	0.244	0	0	0.014	0	0.342
Cl	0.009	0.01	0	0.014	0	0	0.003
Total	97.008	97.042	96.684	97.551	97.92	97.376	98.145
TSi	6.828	7.213	6.849	6.754	6.692	6.984	8.143
TAl	1.172	0.787	1.151	1.246	1.308	1.016	0
Sum_T	8	8	8	8	8	8	8.143
CAl	1.409	1.869	0.509	0.755	0.641	0.393	1.384
CCr	0	0.011	0	0.012	0.002	0.024	0.031
CTi	0.11	0.033	0.067	0.078	0.074	0.052	0.031
CMg	2.557	2.554	2.843	2.549	2.626	3.743	3.554
CFe2	0.924	0.533	1.58	1.605	1.657	0.787	0
Sum_C	5	5	5	5	5	5	5

BMg	0	0	0	0	0	0	0.67
BFe2	1.051	1.438	0.107	0.127	0.133	0.176	1.11
BMn	0.035	0.048	0.017	0.035	0.035	0.018	0.02
BCa	0.914	0.514	1.853	1.792	1.832	1.765	0.199
BNa	0	0	0.022	0.046	0	0.041	0
Sum_B	2	2	2	2	2	2	2
ACa	0.968	1.434	0	0	0.044	0	1.875
ANa	0.646	0.63	0.432	0.484	0.524	0.508	0.528
AK	0.06	0.078	0.093	0.12	0.137	0.023	0.029
Sum_A	1.674	2.142	0.525	0.604	0.705	0.531	2.432
Sum_cat	16.674	17.142	15.525	15.604	15.705	15.531	17.575
CCl	0.002	0.003	0	0.004	0	0	0.001
CF	0.082	0.126	0	0	0.007	0	0.175

Annexure 5: EPMA data of feldspar of Etalin Formation and cations recalculated on the basis of 8 oxygen atoms

Sample No.	**27**	**27**	**30**	**30**	**30**	**30**
Points	27-8/1.	27-9/1.	30-1/1.	30-12/1.	30-26/1.	30-27/1.
SiO2	68.65	68.555	66.39	67.686	63.957	65.242
TiO2	0	0.043	0.06	0.082	0	0
Al2O3	19.786	19.647	19.36	19.09	21.887	21.781
FeO	0.298	0.312	0.102	0.142	0	0.068
MnO	0.033	0	0.004	0	0.007	0.079
MgO	0	0	0.066	0.001	0	0.004
CaO	0.78	0.756	1.175	0.437	3.561	3.02
Na2O	11.528	11.62	10.589	11.568	9.703	9.832
K2O	0	0.064	0.095	0.048	0.086	0.084
BaO	0.05	0.023	0	0	0	0
P2O5	0	0.03	0	0	0	0.028
Cr2O3	0	0.844	0.613	0	0	0
ZnO	0	0	0.016	0	0	0.01
F	0	0.157	0	0	0	0.003
Cl	0.033	0.131	0	0	0.002	0
Total	101.158	102.183	98.47	99.054	99.204	100.151
Si	2.975	2.959	2.957	2.99	2.844	2.868

Al	1.01	0.999	1.015	0.993	1.146	1.127
Fe3						
Ti	0	0.001	0.002	0.003	0	0
Fe2	0.011	0.011	0.004	0.005	0	0.002
Mn	0.001	0	0	0	0	0.003
Mg	0	0	0.004	0	0	0
Ba	0.001	0	0	0	0	0
Ca	0.036	0.035	0.056	0.021	0.17	0.142
Na	0.969	0.972	0.914	0.991	0.837	0.838
K	0	0.004	0.005	0.003	0.005	0.005
Z	1.018	1.022	0.983	1.02	1.012	0.99
Ab	96.4	96.1	93.7	97.6	82.7	85.1
An	3.6	3.5	5.7	2.1	16.8	14.4
Or	0	0.4	0.5	0.3	0.5	0.5

Rocks of Etalin Formation are mainly composed of amphibole, feldspar, quartz, chlorite and mica (Figure 13). Analysis has been done for all the minerals to study the composition of the minerals. All the amphiboles of Etalin Formation shows a wide range of composition [CaO: 0.02-11.957 wt%, MgO: 11.027-28.418 wt%, FeO: 3.88-14.821 wt%]. According to the classification scheme of Leake et al., 1997 the amphiboles are classified (Figure 14 & 15) as Fe-Mg-Mn-Li group [(Ca + Na)B < 1.0, Σ(Fe, Mg, Mn, Li) > 1.0] and calcic group [(Ca + Na)B > 1.0 and NaB < 0.5]. (Ca + Na)B value in Fe-Mg-Mn-Li group and calcic group (Figure 16 & 17) ranges from 0.03 to 0.98 and 1.27 to 1.93, respectively, with Σ(Fe, Mg, Mn, Li) value ranges from 1.01 to 2.04 and 0.06 to 0.7, respectively. TSi value ranges from 6.43 to 9.2 atoms per formula unit (a. p. f. u) whereas AlTot value ranges from 0.01 to 2.65 a. p. f. u. XMg [where XMg = (Mg / Mg + Fe)] value of Fe-Mg-Mn-Li group and calcic group ranges from 0.56 to 0.89 and 0.84 to 0.95, respectively. The amphiboles of Fe-Mg-Mn-Li group are further classified as orthorhombic and monoclinic amphibole. Orthorhombic amphibole shows a composition range from gedrite at core [TSi 6.82 and XMg 0.71 and AlTot 2.58] to anthophyllite at the rim [TSi 7.2 and XMg 0.63 and AlTot 2.65]. Monoclinic amphiboles show a composition of cummingtonite [TSi 7.8-9.2 and XMg 0.78-0.92 and AlTot 0.05 to 1.6]. As most of the samples have TSi values more than 8, it doesn't come within the plot area. Calcic amphiboles are all monoclinic amphibole and their classification parameters according to Leake et al., 1997 are (1) CaB ≥ 1.5; (Na + K)A < 0.5 with CaA < 0.5 and CaA ≥ 0.5 and (2) CaB ≥ 1.5; (Na + K)A ≥ 0.5 with Ti < 0.5 and Ti ≥ 0.5. Calcic amphiboles, according to former classification, ranges from tremolite to magnesiohornblende to tschermakite [TSi 6.5 to 7.9; XMg 0.92-0.98 and AlTot 0.2 to 1.4] and according to latter one, are edenite to pargasite [TSi 6.4 to 7.4; XMg 0.84-0.95 and AlTot 1.4 to 2.6]. In samples of amphibole from core to rim shows a uniform composition [XMg 0.91 to 0.92 and 0.84 to 0.93, Si 6.5 to 6.4 and 49 7.4 to 7.1 and AlTot 2.6 to 2.6 and 1.4 to 1.4, respectively] throughout the grains. This homogeneity is indicative of equilibrium during crystal growth (Spear, 1981). Feldspars has been recalculated and classified on the basis of 8 oxygen atoms and were plotted in Or-Ab-An ternary diagram. Feldspars are rich in Na content that varies from 0.79 to 0.991 and poor in Ca content that varies from 0.012 to 0.178. Feldspar of Etalin Formation varies in between albite to oligoclase. Anthophyllite and gedrite occur in a wide range of rocks of metamorphic and metasomatic rocks. Anthophyllite developed with an asbestiform habit during metamorphism of ultrabasic rock and in this paragenesis it is usually associated with talc (Deer, W. A. et. al., 1977) but in the investigated area talc has not been observed. Cummingtonite is commonly found in amphibolites derived by regional metamorphism from basic igneous rock (Deer, W.A. et al., 1977) and is also associated with common hornblende. Hornblendes is common constituent of regionally metamorphosed rock and is stable from greenschist to the lower part of granulite facies. Anthophyllite, cummingtonite and hornblende is present throughout in banded hornblende chlorite schist as well as hornblende chlorite of Etalin Formation. Hornblende and plagioclase are the main constituent of hornblende schists, hornblende gneisses and amphibolites. This indicates that the protolith of the Etalin Formation is basic in nature. Pargasite are very rich in magnesium is restricted to metamorphosed impure dolomitic limestone and is observed near the contact of carbonatite and banded hornblende chlorite schist. Feldspars of are mostly albitic to oligoclase in composition. Plagioclase having An1-An6.6 in composition are albitic in nature and An14.4-An26.6 in composition are oligoclase in nature. With increase in temperature, composition of plagioclase becomes more Ca rich. Albite is the characteristic mineral of greenschist facies. When the rock prograde from greenschist to amphibolite facies, the first transition is marked by the change in composition from albite to oligoclase. It can be inferred from the feldspar composition that the rock of Etalin Formation has been metamorphosed to amphibolites facies.

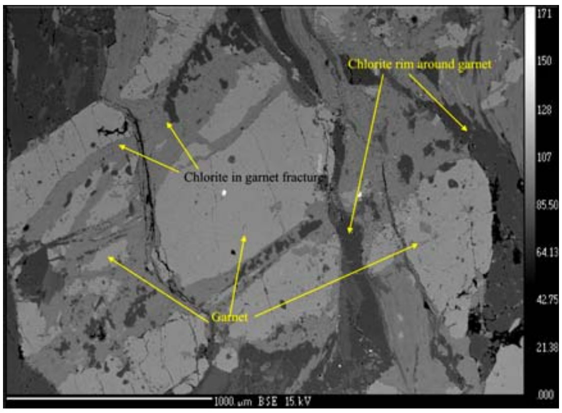

Figure 12: BSE Image of hbl chl Schist Showing Garnet Alteration to Chlorite along the Fractures.

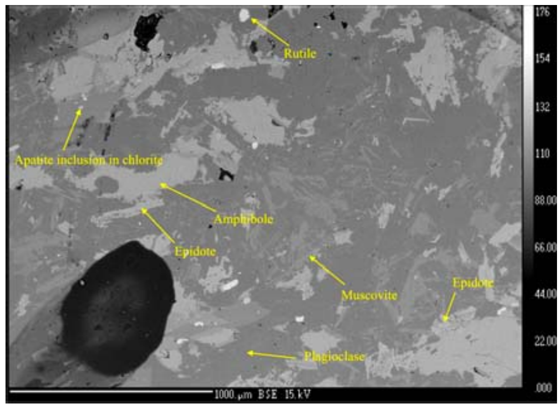

Figure 13: BSE Image of Hornblende Chlorite Schist Showing Mineral Phases.

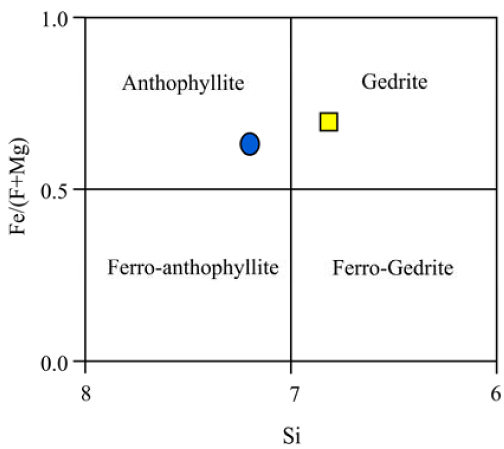

Figure 14: Diagram Showing Classification of Fe-Mg-Mn Amphibole (Orthorhombic) of Etalin Formation after Leake et al., 1991.

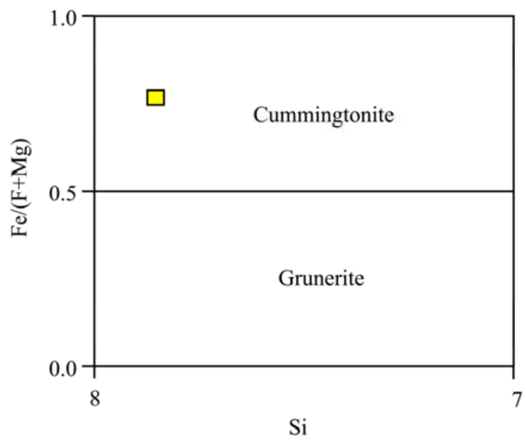

Figure 15: Diagram Showing Classification of Fe-Mg-Mn Amphibole (Monoclinic) of Etalin Formation after Leake et al., 1991.

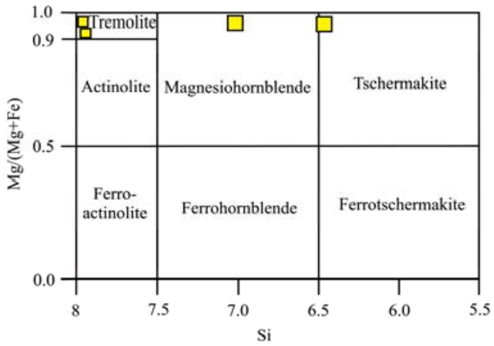

Figure 16: Diagram Showing Classification of Calcic Amphiboles of Etalin Formation according to the Parameter $Ca_B \geq 1.5$; $(Na + K)_A < 0.5$ with $Ca_A < 0.5$ and $Ca_A \geq 0.5$.

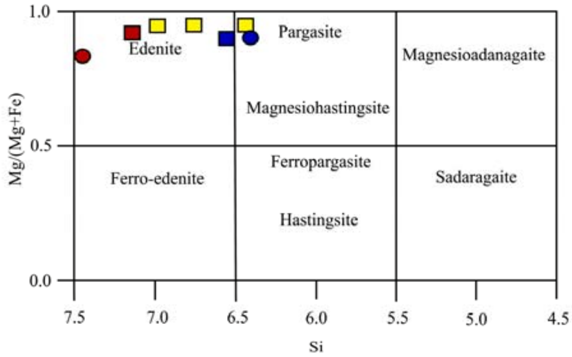

Figure 17: Diagram Showing Classification of calcic Amphiboles of Etalin Formation according to the Parameter $Ca_B \geq 1.5$; $(Na + K)_A \geq 0.5$ with $Ti < 0.5$ and $Ti \geq 0.5$

Conclusion

Etalin Formation is one of the important geological unit in trans Himalayan Belt on Cretaceous-Tertiary age. Etalin Formation comprises metasediments represented by interbanded sequence of migmatitic gneiss, calc silicate gneiss, marble, quartzite, mica schist and amphibolite. Amphibolite is one of the major constituents of the Etalin formation. Hornblende chlorite schist of Etalin Formation were plotted on total alkali vs silica diagram and classified as basaltic- andesite composition. The rocks of Etalin Formation show calc alkaline nature when plotted in AFM diagram. According to Shand's Index, the composition of Etalin Formation is dominantly metaluminous having A/NK value (molar) ranges from 1.4 to 2.45 and A/CNK value (molar) ranges from 0.17 to 1.17. Trace elements discrimination diagram has been used to infer the tectonic environment of the rock. Rock of Etalin Formation were plotted in Hf/3-Th-Ta triangular diagram after and it plotted in D field which indicate that these are calc alkaline basalt. Furthermore, it is also plotted in TiO2-MnOx10-P2O2x10 triangular diagram which also represent that these are calcalkaline basalt. These calc alkaline basalts decipher the tectonic setting of theses basalts as volcanic arc setting. In multi element plot, elements are arranged into LILE group followed by HFSE group ultimately followed by transition element Ni and Cr, from left to right. The pattern shows enrichment in LIL elements which may be due to the involvement of fluid phase and the enrichment of Th and Ba are indicative, but not diagnostic, of basalts that have experienced crustal contamination. The REE data were normalised to MORB values and are presented on a concentration vs atomic number diagram. The REE pattern shows enriched LREE pattern with almost a linear trend from La-Nd with a moderate Eu anomaly whereas the HREE (Er to Lu) shows fractionated pattern. Distribution pattern of REE exhibits medium to strongly fractionated pattern with (La/Yb)N ratio 1.56 to 12.83 with almost flat LREE pattern with (La/Sm)N ratio 42 0.55 to 1.61 and low to moderately enriched HREE pattern with (Tb/Yb)N ratio 0.98 to 4.28. The total average REE content is 57.14. REE pattern exhibits medium to strong Eu anomaly with Eu/Eu* value ranges from 0.71 to 0.15 which may be attributed to the presence of feldspar in the parent rock.

Acknowledgement

The authors are thankful to the Director General, Geological Survey of India, for his permission to publish this manuscript. Authors are thankful to all the higher officials who supported us during the project works for their administrative and technical supports. The author also express thanks to the officers and staffs of Petrology- especially EPMA laboratories of NCEGR Faridabad. Smt. Pushp Lata, Dy.Director General, NCEGR, Faridabad is gratefully acknowledged for her valuable support in preparing this manuscript.

References

[1] Bevins, R. E., Kokelaar, B. P. and Dunkley, P. N. 1984: Petrology and geochemistry of lower to middle Ordovician igneous rocks in Wales: a volcanic arc to marginal basin transition. Proc. Geol. Ass. 95, 337-347.
[2] Deer, W. A., Howie, R. A. and Zussman, J. 1966: An introduction to the rock forming minerals. Longman Scientific and Technical press.
[3] Irvine, T. N. & Baragar, W. R. (1971): A guide to the chemical classification of the common igneous rocks. Canadian Journal of Earth Sciences 8, 523–548.
[4] Kirmani, I. R., Ahmed, S., Tangri, S. K. and Raut, P. K. (1987): Geology of the area around Hayuliang-Chirangla-Yatong, Lohit district, Arunachal Pradesh. Geol. Surv. of India. Progress Report (unpublished) FS-1985-86.
[5] Le Bas, M. J., Le Maitre, R. W., Streckeisen, A. and Zanettin, B., 1986: A chemical classification of volcanic rocks based on total alkali-silica diagram. Journal of Petrology 27, pp. 745-750.
[6] Leake, B. E., Woolley, A. R., Arps, C. E. S., Birch, W. D., Gilbert, M. C., Grice, J. D., Hawthorne, F. C., Kato, A., Kisch, H. J., Krivovichev, V. G., Linthout, K., Laird, J., Mandarino, J. A., Maresch, W. V., Nickel, E. H., Rock, N. W. S, Schumacher, J. C., Smith, B. C., Stephenson, N. C. N., Ungaritti, L., Whittaker, E. J. W. and Guo, Y., 1997: Nomenclature of amphiboles: Report of the Subcommittee of Amphiboles of the International 59 Minerological Association, Commission on New Minerals and Mineral Names. American Mineralogists 82, pp. 1019-1037.
[7] Nandy, D. R. (1980): Tectonics patterns in northeast India. Ind Jour. Earth Sci., v 7(1), pp.103-107.
[8] Philpotts, R. A. (1989). Petrography of igneous and metamorphic rocks. Pearson Education, Inc.
[9] Shand, S.J.(1943). The Eruptive Rocks, 2nd edition. New York: John Wiley, pp. 444.
[10] Singh, S. (1993): Geology and tectonics of the eastern syntaxis bend, Arunachal Himalaya: Journal of Himalayan Geology, v 4, pp. 149-163.
[11] Spear F. S. (1981): An experimental study of hornblende stability and compositional variability in amphibolite. American Journal of Science, 281, 697.734.
[12] Taylor, S. R. and McLennan, S. M., 1985: The continental crust: its composition and evolution. Blackwell, Oxford.
[13] Wood, D. A, 1980: The application of Th-Hf-Ta diagram to problems of tectonomagmatic classification and to establishing the nature of crustal contamination of basaltic lava of the British Tertiary volcanic province. Earth Planet Sci. Lett. 50, pp 11-30.